

Experimental results on synchronization times and stable states in locally coupled light-controlled oscillators

BY NICOLAS RUBIDO¹, CECILIA CABEZA^{1,*}, ARTURO C. MARTÍ¹
AND GONZALO MARCELO RAMÍREZ ÁVILA²

¹*Instituto de Física, Universidad de la República, Montevideo, Uruguay*

²*Instituto de Investigaciones Físicas, Universidad Mayor de San Andrés,
Casilla 8635, La Paz, Bolivia*

Recently, a new kind of optically coupled oscillators that behave as a relaxation oscillator has been studied experimentally in the case of local coupling. Even though numerical results exist, there are no references about experimental studies concerning the synchronization times with local coupling. In this paper, we study both experimentally and numerically a system of coupled oscillators in different configurations, including local coupling. Synchronization times are quantified as a function of the initial conditions and the coupling strength. For each configuration, the number of stable states is determined varying the different parameters that characterize each oscillator. Experimental results are compared with numerical simulations.

Keywords: synchronization times; local coupling; networks

1. Introduction

Synchronization is a common feature of oscillatory systems and may be understood as an adjustment of rhythms of self-sustained oscillators due to their weak interaction (Schäfer *et al.* 1999). Synchronization is an ubiquitous phenomenon and nowadays is a widely spread topic. Several books have been devoted to this subject both from rigorous (Pikovsky *et al.* 2001, 2003; Manrubia *et al.* 2003) and popularization point of view (Strogatz 2003). Different kinds of systems show synchronous behaviour varying from biological (Glass 2001; Kreuz *et al.* 2007), chemical (Neu 1980; Fukuda *et al.* 2005) and ecological (Blasius *et al.* 1999) to electronic devices (Chua 1993; Murali *et al.* 1995; Kittel *et al.* 1998; Cosp *et al.* 2004; Pisarchik *et al.* 2008). Among the different types of models that have been considered to study synchronization, we could mention coupled maps (Masoller *et al.* 2003; Masoller & Marti 2005; Morgul *et al.* 2008), Kuramoto model (Acebron *et al.* 2005; Chen *et al.* 2008) and relaxation

* Author for correspondence (cecilia@fisica.edu.uy).

One contribution of 16 to a Theme Issue ‘Topics on non-equilibrium statistical mechanics and nonlinear physics’.

oscillators (Campbell *et al.* 2004), in particular pulse-coupled oscillators (Mirollo & Strogatz 1990; Bottani 1995). In this respect, the integrate-and-fire model is one of the most studied and it has been studied analytically (Timme *et al.* 2002) and numerically (Corral *et al.* 1995). On the other hand, few experimental works have been reported concerned to this type of oscillators. Light-controlled oscillator (LCO) is a realistic pulse oscillator whose behaviour resembles to the integrate-and-fire oscillator but differs by the fact that the discharge is not instantaneous (Guisset *et al.* 2002). The experimental results concerning the LCOs have devoted to local coupling configurations (Ramírez Ávila *et al.* 2003). Transients or synchronization times in different sort of systems have attracted the attention of several scientists, but they do not so far seem to have made significant progress in its analysis and only numerical results have been reported (Politi *et al.* 1993; Acebron & Bonilla, 1998; Fukai & Kanemura, 2000; Bagnoli & Ceconi, 2001; Zumdieck *et al.* 2004). Concerning the LCOs' synchronization times, numerical results for local and global coupling configurations have been reported (Ramírez Ávila *et al.* 2006, 2007). This paper deals with the experimental determination of the synchronization times in LCOs as a function of the initial conditions and the coupling topology.

2. Light-coupled oscillator setup

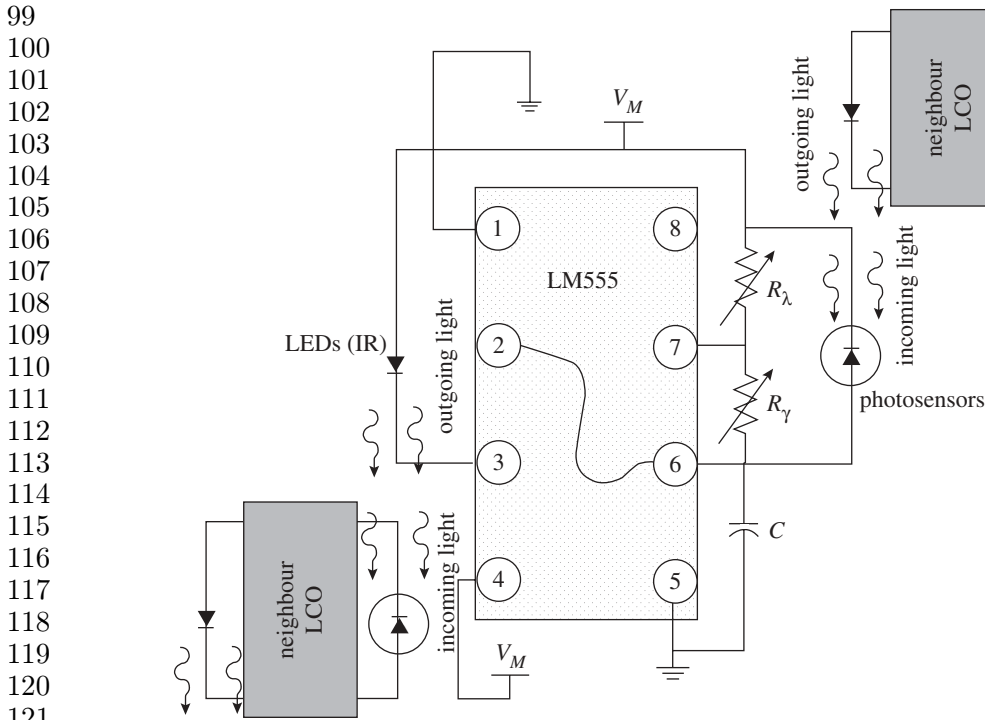
The LCO used in this work is an open electronic version of an oscillator that mimics gregarious fireflies. Basically, the LCO is composed of an LM555 chip to function in an astable oscillating mode (Ramírez Ávila *et al.* 2003). It possesses an intrinsic period and pulse-like IR light emissions, both of them can be manually modified on the spot enabling quantitative measurement of phase differences and period variations with the required precision.

The dual RC circuit (figure 1) was mounted on a 8×5 cm proto-board. The characteristic frequencies, named λ and γ , corresponding to the charging and discharging stages of the capacitor C , respectively, are determined when no external perturbation is done. The timing components are set due to two variable resistors, R_λ and R_γ , so the intrinsic longer charging period can be changed by acting on R_λ , and flashing can be widened by modifying the discharging stage, thus, R_γ . Coupling is achieved by photosensor diodes connected in parallel, which act as current sources when they are receiving IR light, shortening the charging time and making a longer discharging stage. When all photosensors are masked, namely in dark, the periods only depend on the electronics. An LM555 constitutes the brain of the electronic firefly, managing these current deviations and setting the maximum charging and minimum discharging voltages to 2/3 and 1/3 of the source voltage, correspondingly.

In our model, the resistors were changed through the different configurations used to ensure synchronization when coupling strength was small, though the values used were usually set to be almost identical between oscillators. Typical values are:

$$R_\lambda = [58.7 - 73.4] \pm 0.1 \text{ k}\Omega,$$

$$R_\gamma = [1.00 - 1.30] \pm 0.01 \text{ k}\Omega.$$



122 Figure 1. Simplified block diagram of the LCO and schematic view of the coupling between LCOs.
123
124

125 These specific values are those used when coupling of two LCOs by mutual
126 interaction was held. The ratio between these two resistors was always set smaller
127 than 2.5 per cent in order to keep the pulse-like light emission hypothesis that
128 mimics its biological analogue. Using a $0.47\ \mu\text{F}$ capacitor, the natural periods
129 are $T_\lambda = 27.6\ \text{ms}$ and $T_\gamma = 0.43\ \text{ms}$. The voltage source being a 9 V battery, the
130 LM555 sets the lower and upper threshold voltages of the RC circuit to 3 and
131 6 V, respectively. The coupling strength is changed varying the distance between
132 the LCOs and can also be changed by placing different resistors in series with
133 the diodes. The temporal signals in the capacitors were acquired using a NI-
134 USB 6215 data acquisition device. The characteristic frequency of the LCO was
135 calculated using standard FFT algorithm. In figure 2, a typical temporal signal
136 and a spectrum are shown corresponding to the master LCO before coupling.

137 Master-Slave (MS) and mutual interaction (MI) were used in this work. In
138 the MS configuration, one LCO is in dark and it is namely the master, LCO1;
139 the other LCO, namely the slave, LCO2, can be excited through the light-pulsed
140 emitted by the LCO1. In the MI configuration, both LCOs have the same mutual
141 influence; they act on each other in the same way with equal strength, so they are
142 interchangeable. In order to study the influence of the coupling parameter on the
143 synchronization time, we vary the distance between the IR diode and the photo-
144 sensor. We have used $d_1 = 5.0\ \text{cm}$, $d_2 = 10.0\ \text{cm}$, $d_3 = 15.0\ \text{cm}$ and $d_4 = 25.0\ \text{cm}$.
145 In addition, for a fixed distance, we vary the current on the IR diode, which
146 implies that we can increase the current in a way that the coupling parameter is
147 duplicated. The experimental setup is shown in figure 3.

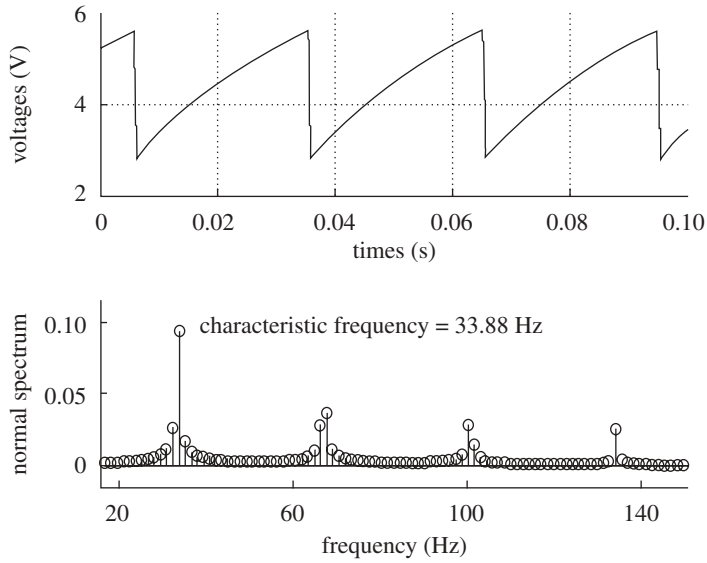


Figure 2. Temporal signal (upper) and normal spectrum (bottom) corresponding to the master LCO before coupling.

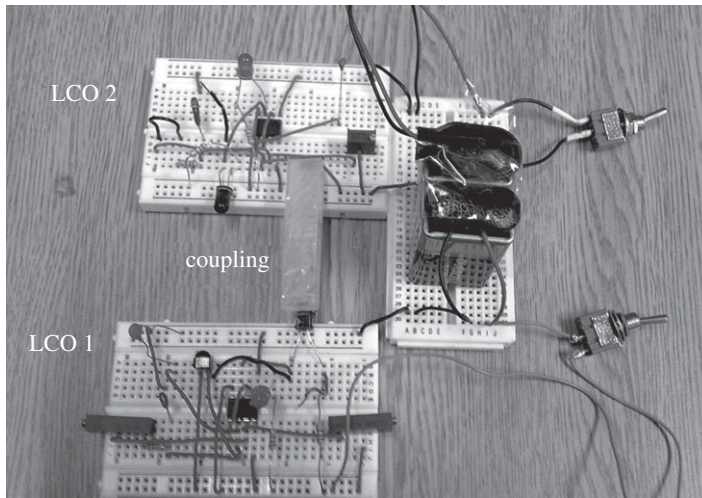


Figure 3. Experimental setup corresponding to a master–slave (MS) configuration and a separation of $d_1 = 5.0$ cm.

3. Experimentally determined synchronization times

As a system of LCOs can be modelled by a set of ordinary differential equations, see §4, initial conditions play an important role determining which solutions will correspond to the oscillator's evolution. When coupling is taken into account, particular solutions are modified due to the appearance of a connection matrix,

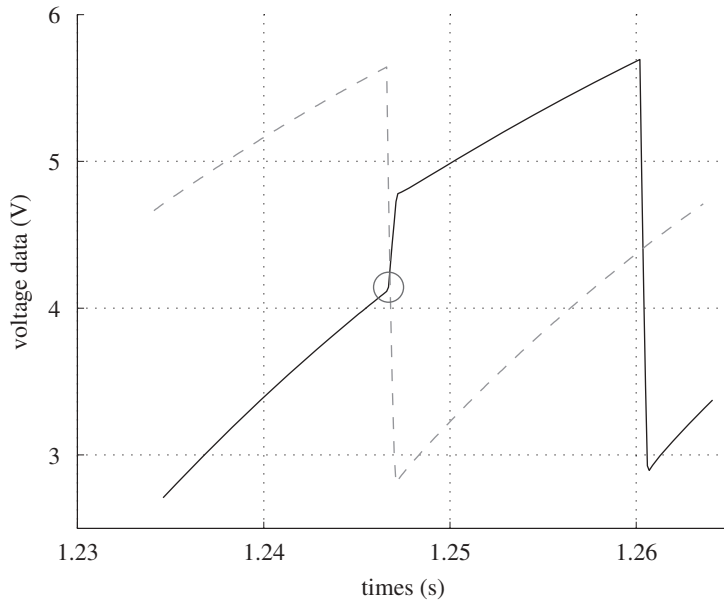


Figure 4. Perturbation acting upon charging stage in a slave LCO. Gray dotted line corresponds to master LCO and black line corresponds to slave LCO. The circle indicates the start of the perturbation.

linking the equations. Solutions are now, not only, initial conditions-dependent, but they are also a function of how coupling is set, meaning, that it matters what configuration and coupling strength is implemented. Nevertheless, in all cases, the frequency at which flashes occur, corresponding to the discharging stage of the RC circuit, can be considered as a basic feature of an LCO.

(a) Phase locking and frequency entrainment

As perturbations due to other LCOs do not modify the oscillating amplitudes, the coupling between oscillators imposes a relation between their characteristic frequencies. By means of an external periodic perturbation, frequency entrainment is possible and as a consequence, LCOs. The latter occurs due to the fact that any external (pulse-like in our case) perturbation acting upon an oscillator will increase the capacitor charge, causing modifications in its charging or discharging stage, depending where it is held. Thus, if the perturbation acts during the charging stage, it will increase the LCO frequency, and if it acts upon the discharging stage, it will decrease its characteristic frequency. In figure 4 charge–discharge cycle is shown, corresponding to MS configuration.

The frequency entrainment that happens when LCOs are coupled can be quantified determining period variations in time. By choosing a reference period T^* , we can define a phase difference for each LCO as:

$$\Delta\Phi_i = \left(1 - \frac{T_i(\Phi)}{T^*}\right),$$

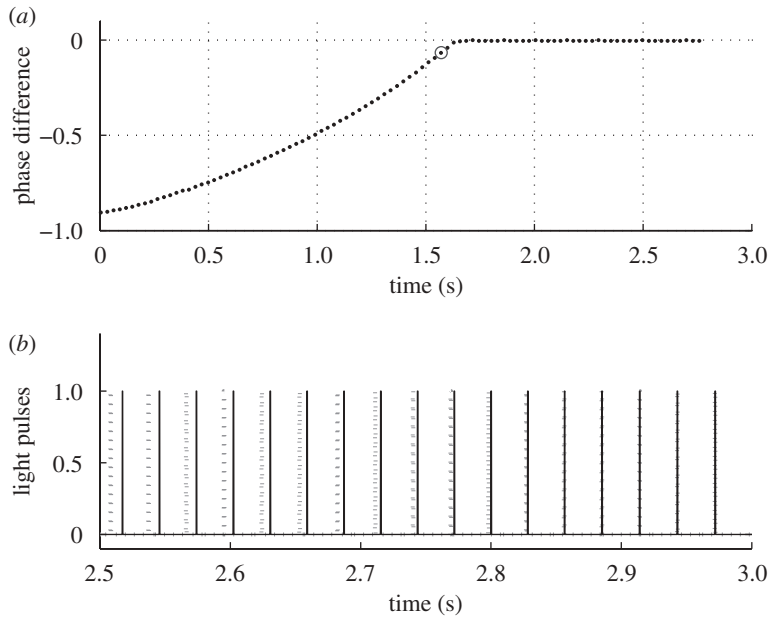


Figure 5. (a) Phase difference between oscillators. (b) IR light pulses in each LCOs.

where $T_i(\phi)$ represents the new period of the oscillator being perturbed. The phase difference between LCOs can be defined as:

$$\Delta\Phi_{ij} = \Delta\Phi_i - \Delta\Phi_j.$$

When constant phase difference is achieved, oscillators are synchronized.

Taking the maximum charging voltage as our reference for choosing the LCO period, we could qualify two different behaviours towards synchronization: positive phase difference and negative phase difference. The first one corresponds to a shortening of the free-running period T_λ , which only means that perturbation acts as a positive feedback through the charging stage. A lower phase-locking limit is achieved when the duration of the perturbation is not sufficient anymore to reach the switching point of λ towards γ . As a consequence, this case is a stable situation. In figure 5, we can observe the temporal evolution of the phase difference and IR light pulses in the MS configuration. At $t = 1.61$ s, the phase difference becomes zero, i.e. the LCOs are synchronized and the IR pulses are emitted at unison. When phase difference is negative, it means that perturbation acts to widen γ , consequently the period is increased and the phase-locking should be stable. However, this influence is of little importance because the discharge current is usually two orders of magnitude greater than the photocurrent (except figure 4 where the coupling strength was set greater by electronic changes), and also, perturbation width is of the order of 0.02λ . As a consequence, the upper limit is reached as soon as the photocurrent shortens the next charging stage resulting in an unstable situation.

Figure 6 shows the evolution of the trajectories in phase space for two identical coupled LCOs, where LCO1 was set as reference.

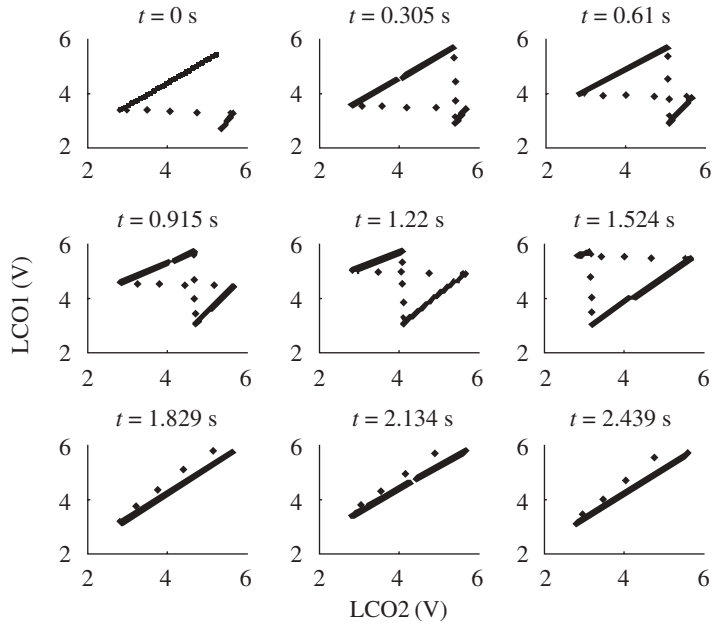


Figure 6. Evolution of phase space trajectories for two identical coupled LCOs.

(b) Different initial conditions

Now the quantification of synchronization times by means of constant phase differences is possible; we start dealing with initial conditions. Experimentally, by leaving the LCO1 on, we managed to control coupling by switching on the other LCOs afterwards and thus, we found a way of creating different initial conditions and record their corresponding synchronization times, obtaining behaviours like those shown in figure 7. Nevertheless, this way of proceeding gives rise to random initial conditions for both LCOs in every measurement.

The initial condition for LCO2 was recorded as the voltage corresponding to the first IR lightning from the other. This was done because, where this value is located will matter directly to the time that LCOs will take to synchronize, meaning that it determines which phase-locking situation rules the evolution of the system.

(c) Stable configurations

In addition, with the aim of increasing the coupling strength electronically, we place a greater photocurrent (this is done by changing the resistors connected in series with the diodes), we can obtain different connection matrices corresponding to different types of networks. As mentioned through §2, these matrices are: the symmetric MI and asymmetric MS configurations. For each configuration, coupling strength was changed by placing LCOs further apart. Then, coupling strength was changed electronically, thus, increasing perturbation influence, and the procedure was repeated. Figures 8 and 9 display typical behaviours for a coupling strength that corresponds to the one shown in figure 7, where differences

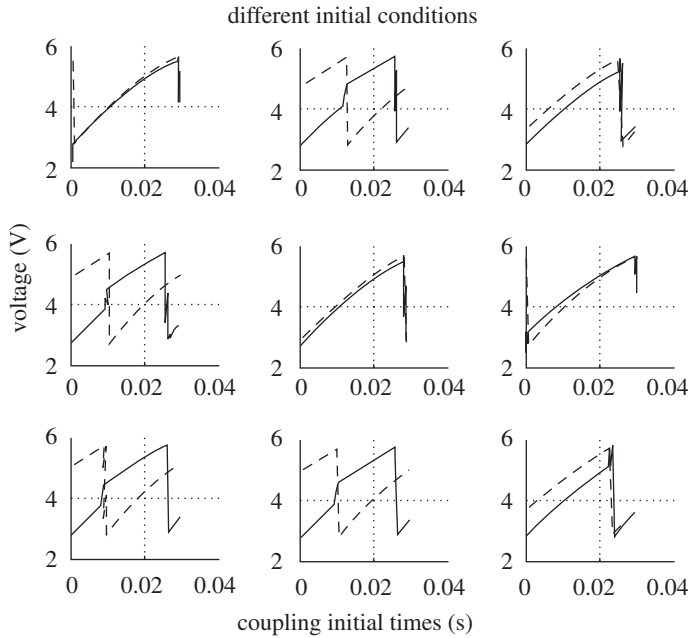


Figure 7. Different initial conditions generated when LCO2 is turned on.

between synchronization curves within these figures are visible on the times LCOs take to approach synchronization, thus, their slope.

When comparing different distances, figure 10, the curves for each configuration exhibit similar shapes. Thus, synchronization times depend on the coupling strength in a way that once the coupling strength is fixed, the system will locate itself, for different initial conditions, within the corresponding curve.

4. Numerical method

LCOs might be described by a simple model consisting of a set of differential equations that take into account the charging and discharging stages due to the RC circuits and the flip-flop LM555; this last element establish well-defined thresholds for the RC circuit charging at $2V_M/3$ and at $V_M/3$ for the RC circuit discharging, where V_M is the source voltage value which takes the value 9V because in experimental work we use simple batteries as it has been stated in § 2. The equations that describe the coupled LCOs are:

$$\begin{aligned} \frac{dV_i(t)}{dt} = & \lambda_i[(V_{Mi} - V_i(t)]\epsilon_i(t) - \gamma_i V_i(t)[1 - \epsilon_i(t)] \\ & + \sum_{i,j}^N \beta_{ij} \delta_{ij} [1 - \epsilon_j(t)], \quad i, j = 1, \dots, N, \end{aligned} \quad (4.1)$$

where β_{ij} is the coupling strength, $\delta_{ij} = 1$ if the LCOs interact and $\delta_{ij} = 0$ otherwise, and $\epsilon_i(t)$ is the oscillator state that takes the value 1 (charging stage) or

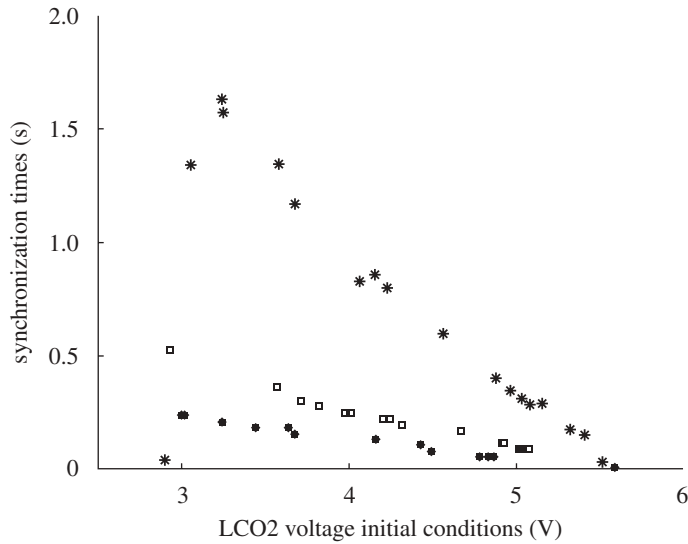


Figure 8. Synchronization times as a function of the initial conditions, corresponding to MS configuration and different distances. Filled circle, 10 cm; open box, 15 cm; star, 25 cm.

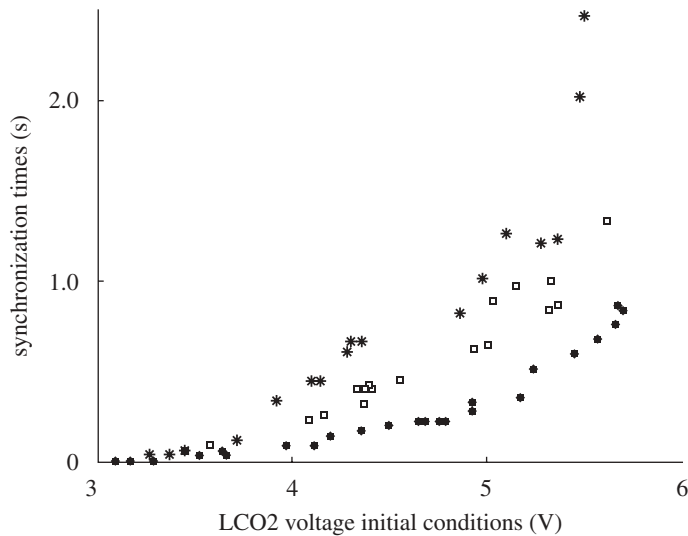


Figure 9. Synchronization times as a function of the initial voltage, corresponding to MI configuration and different distances. Filled circle, 10 cm; open box, 15 cm; star, 25 cm.

0 (discharging stage); $\epsilon_i(t)$ changes its value when it achieves the upper threshold ($2V_M/3$) or the lower threshold ($V_M/3$). We must mention that this model has been validated experimentally (Ramírez Ávila *et al.* 2003).

Numerical results for the two configurations used when LCO1 initial condition is 3 V are shown in figures 11–13. Figures 14 and 15 show the comparison between experimental and numerical results. Clearly, we can observe a good agreement with them.

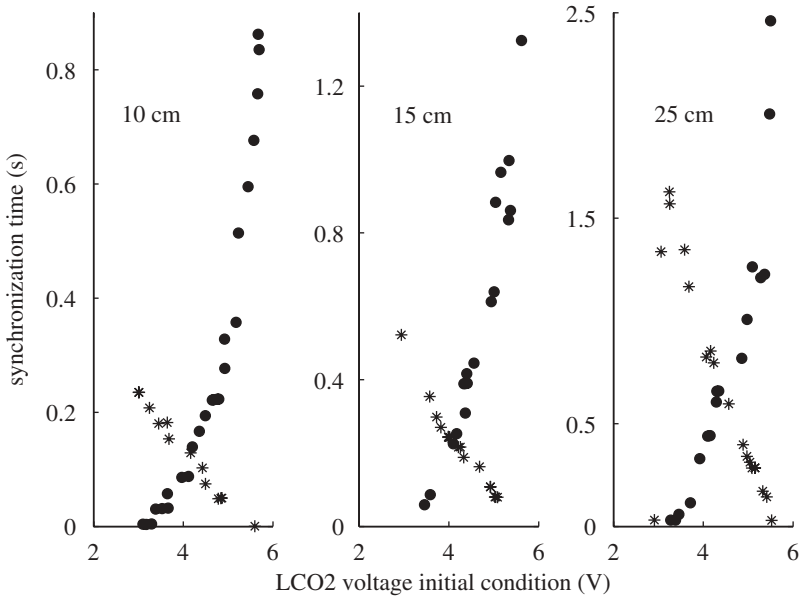


Figure 10. Comparison of synchronization times as function of the initial conditions corresponding to MS and MI configurations and different distances. Circles correspond to MI and stars to MS.

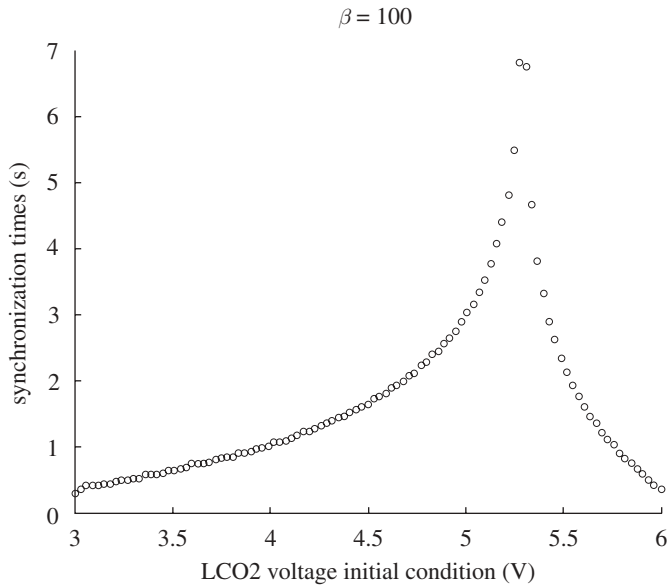
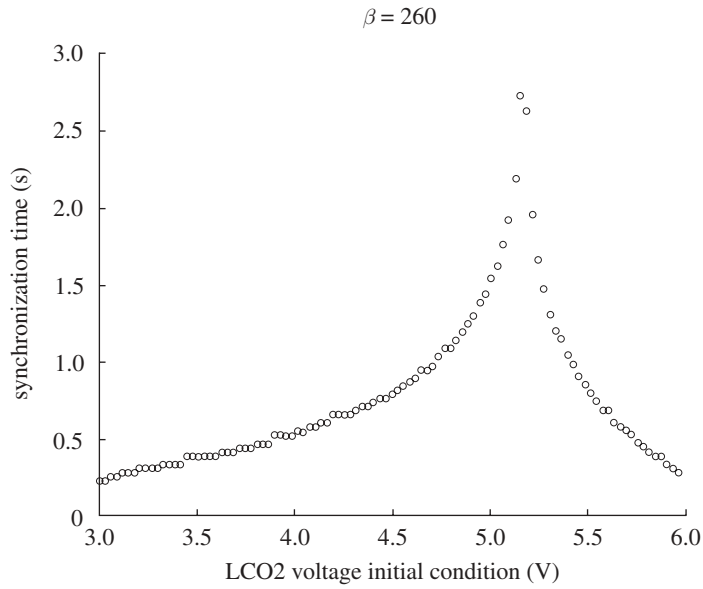
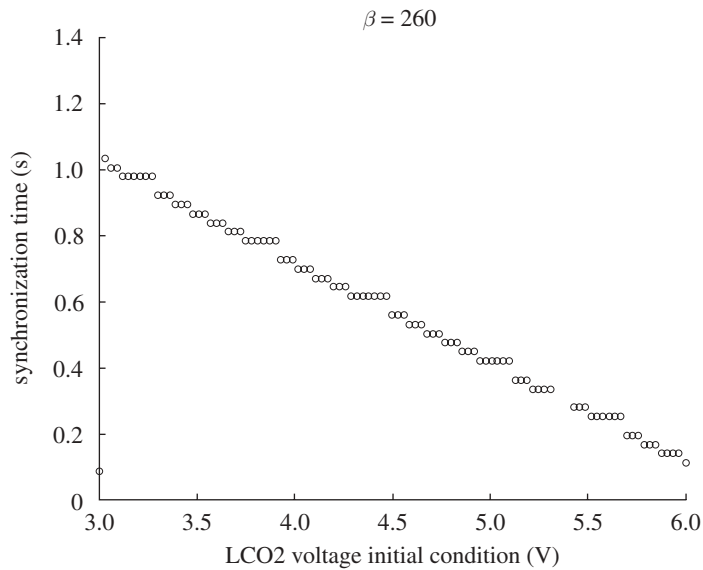


Figure 11. Synchronization times as a function of the initial conditions for MI configuration and $\beta = 100$.



510 Figure 12. Synchronization times as a function of the initial conditions for MI configuration
511 and $\beta = 260$.



536 Figure 13. Synchronization times as a function of the initial conditions for MS configuration
537 and $\beta = 260$.

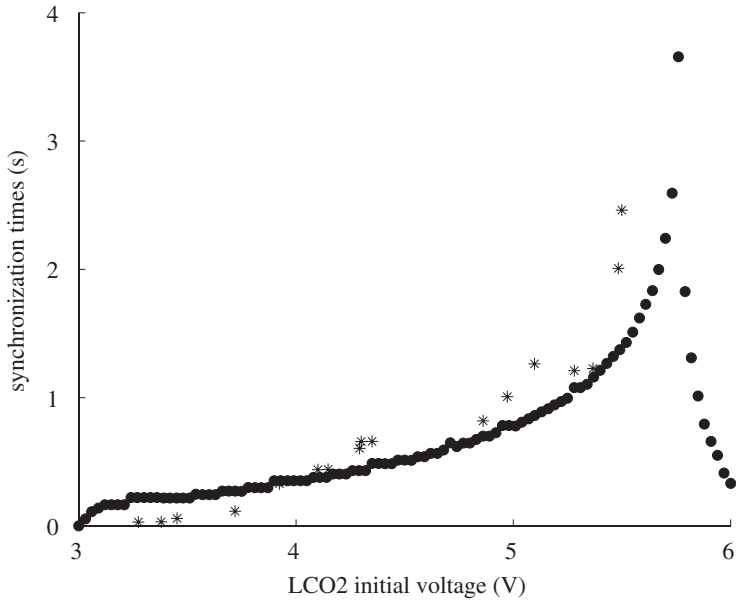


Figure 14. Comparison between numerical and experimental results for MI configuration, corresponding to $\beta = 160$ and $d_4 = 25.0$ cm, respectively. Filled circle, numerical data; asterisk, experimental data.

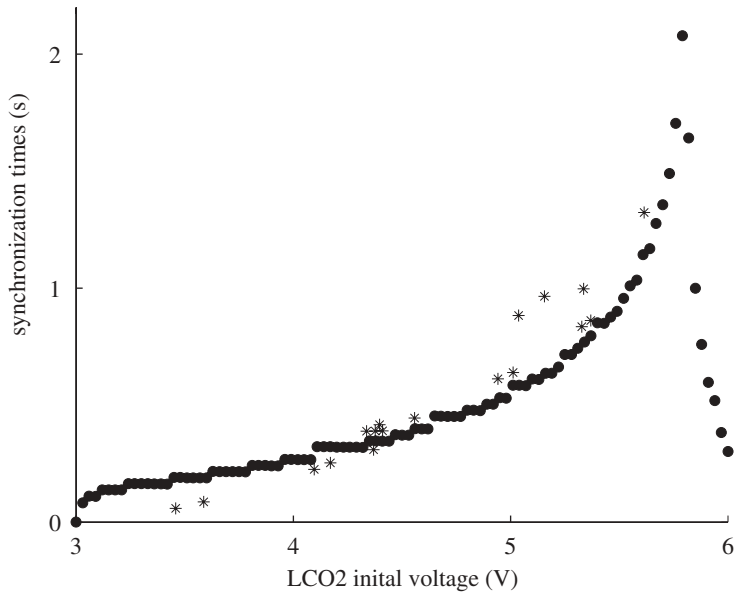


Figure 15. Comparison between numerical and experimental results for MI configuration, corresponding to $\beta = 230$ and $d_3 = 15.0$ cm, respectively. Filled circle, numerical data; asterisk, experimental data.

589
590
591
592
593
594
595
596
597
598
599
600
601
602
603
604
605
606
607
608
609
610
611
612
613
614
615
616
617
618
619
620
621
622
623
624
625
626
627
628
629
630
631
632
633
634
635
636
637

5. Conclusions

Through our work, we checked that the LCOs designed had a great resemblance with the behaviour predicted by the model. Furthermore, this design allowed us to modify on the spot their intrinsic period and pulse-like IR light emissions, enabling quantitative measurement of phase differences and period variations with fine precision, and produce electronically different coupling strengths. Synchronization times for two LCOs interacting in MS and MI configuration were found experimentally as well as numerically.

The effect of the coupling strength was analysed in detail. Experimentally, the strength of the coupling was changed forcing greater IR light emissions by changing resistors in series with the photodiodes and by placing LCO at different distances from each other. Comparing simulations with experimental data, we could see behaviours very much alike for synchronization times versus initial conditions, and by doing so, we have also found a way of quantifying the experimental coupling strength. Insight and facilities gained through this experimental work allow us in the future to tackle other aspects of the system, in particular those related to complex networks coupling, synchronization times for different networks, and also analyse the multistability patterns that arise for different initial conditions when more LCOs are interacting.

We acknowledge financial support from PEDECIBA (PNUD URU/06/004, Uruguay), CSIC (U. de la República, Uruguay). G.M.R.A acknowledges Jean-Louis Deneubourg and the Unit of Social Ecology of the Université Libre de Bruxelles.

References

- Acebron, J. A. & Bonilla, L. L. 1998 Asymptotic description of transients and synchronized states of globally coupled oscillators. *Physica D* **114**, 296–314. (doi:10.1016/S0167-2789(97)00197-8)
- Acebrón, J. A., Bonilla, L. L., Pérez Vicente, C. J., Ritort, F. & Spigler, R. 2005 The Kuramoto model: a simple paradigm for synchronization phenomena. *Rev. Mod. Phys.* **77**, 137–185.
- Bagnoli, F. & Ceconi, F. 2001 Synchronization of non-chaotic dynamical systems. *Phys. Lett. A* **282**, 9–17. (doi:10.1016/S0375-9601(01)00154-2)
- Blasius, B., Huppert, A. & Stone, L. 1999 Complex dynamics and phase synchronization in spatially extended ecological systems. *Nature* **399**, 354–359. (doi:10.1038/20676)
- Bottani, S. 1995 Pulse-coupled relaxation oscillators: from biological synchronization to self-organized criticality. *Phys. Rev. Lett.* **74**, 4189–4193. (doi:10.1103/PhysRevLett.74.4189)
- Campbell, S. R., Wang, D. & Jayaprakash, C. 2004 Synchronization rates in classes of relaxation oscillators. *IEEE Trans. Neural Networks*. **15**, 1027–1038. (doi:10.1109/TNN.2004.833134)
- Chen, M., Shang, Y., Zou, Y. & Kurths, J. 2008 Synchronization in the Kuramoto model: a dynamical gradient network approach. *Phys. Rev. E* **77**, 027101–027104. (doi:10.1103/PhysRevE.77.027101)
- Chua, L. O. 1993 Complex dynamics and phase synchronization in spatially extended ecological systems. *J. Circ. Syst. Comp.* **3**, 93–108.
- Corral, A., Prez, C. J., Daz-Guilera, A. & Arenas, A. 1995 Self-organized criticality and synchronization in a lattice model of integrate-and-fire oscillators. *Phys. Rev. Lett.* **74**, 118–121. (doi:10.1103/PhysRevLett.74.118)
- Cosp, J., Madrenas, J., Alarcón, E., Vidal, E. & Villar, G. 2004 Synchronization of nonlinear electronic oscillators for neural computation. *IEEE Trans. Neural Networks*. **15**, 1315–1327. (doi:10.1109/TNN.2004.832808)
- Fukai, T. & Kanemura, S. 2000 Precisely timed transient synchronization by depressing synapses. *Neurocomputing*. **32–33**, 133–140. (dot:10.1016/S0925-2312(00)00154-5)

- 638 Fukuda, H., Morimura, H. & Kai, S. 2005 Global synchronization in two-dimensional
639 lattices of discrete Belousov-Zhabotinsky oscillators. *Physica D* **205**, 80–86. (doi:10.1016/
640 j.physd.2005.01.007)
- 641 Glass, L. 2001 Synchronization and rhythmic processes in biology. *Nature* **410**, 277–284.
642 (doi:10.1038/35065745)
- 643 Guisset, J. L., Deneubourg, J. L. & Ramírez Ávila, G. M. 2002 The phase information associated
644 to synchronized electronic fireflies. (arXiv.nlin.AO/0206036)
- 645 Kittel, A., Parisi, J. & Pyragas, K. 1998 Generalized synchronization of chaos in electronic circuit
646 experiments. *Physica D* **112**, 459–471. (doi:10.1016/S0167-2789(97)00186-3)
- 647 Kreuz, T., Mormann, F., Andrzejak, R. G., Kraskov, A., Lehnertz, K. & Grassberger, P. 2007
648 Measuring synchronization in coupled model systems: a comparison of different approaches.
649 *Physica D* **225**, 29–42. (doi:10.1016/j.physd.2006.09.039)
- 650 Manrubia, S. C., Mikhailov, A. S. & Zanette, D. H. 2003 *Emergence of dynamical order*. Singapore:
651 World Scientific Publishing.
- 652 Masoller, C. & Martí, A. C. 2005 Random delays and the synchronization of chaotic maps. *Phys.*
653 *Rev. Lett.* **94**, 134102–134104. (doi:10.1103/PhysRevLett.94.134102)
- 654 Masoller, C., Martí, A. C. & Zanette, D. H. 2003 Synchronization in an array of globally coupled
655 maps with delayed interactions. *Physica A* **325**, 186–191. (doi:10.1016/S0378-4371(03)00197-3)
- 656 Mirollo, R. E. & Strogatz, S. H. 1990 Synchronization of pulse-coupled biological oscillators. *SIAM*
657 *J. Appl. Math.* **50**, 1645–1662.
- 658 Morgul, O. 2008 On the synchronization of logistic maps. *Phys. Lett. A.* **247**, 391–396.
659 (doi:10.1016/S0375-9601(98)00576-3)
- 660 Murali, K., Lakshmanan, M. & Chua, L. O. 1995 Controlling and synchronization of chaos
661 in the simplest dissipative non-autonomous circuit. *Int. J. Bifurcation Chaos* **5**, 563–571.
662 (doi:10.1142/S0218127495000466)
- 663 Neu, J. C. 1980 Large populations of coupled chemical oscillators. *SIAM J. Appl. Math.* **38**, 305–316.
664 (doi:10.1137/0138026)
- 665 Pikovsky, A. & Maistrenko, Y. (eds) 2003 *Synchronization: theory and application*. Dordrecht, The
666 Netherlands: Kluwer Academic Publishers.
- 667 Pikovsky, A., Rosenblum, M. & Kurths, J. 2001 *Synchronization: a universal concept in nonlinear*
668 *sciences*. New York, NY: Cambridge University Press.
- 669 Pisarchik, A. N., Jaimes-Reátegui, R. & García-López, J. H. 2008 Synchronization of multistable
670 systems. *Int. J. Bifurcation Chaos* **18**, 1801–1819. (doi:10.1142/S0218127408021385)
- 671 Politi, A., Livi, R., Oppo, G. L. & Kapral, R. 1993 Unpredictable behaviour in stable systems.
672 *Europhys. Lett.* **22**, 571–576. (doi:10.1209/0295-5075/22/8/003)
- 673 Ramírez Ávila, G. M., Guisset, J. L. & Deneubourg, J. L. 2003 Synchronization in light-controlled
674 oscillators. *Physica D* **182**, 254–273.
- 675 Ramírez Ávila, G. M., Guisset, J. L. & Deneubourg, J. L. 2006 Synchronization and transients in
676 locally coupled light-controlled oscillators. [in Spanish]. *Rev. Bol. Fis.* **12**, 1–7.
- 677 Ramírez Ávila, G. M., Guisset, J. L. & Deneubourg, J. L. 2007 Synchronous behavior in globally
678 pulse coupled identical relaxation oscillators. [in Spanish]. *Rev. Bol. Fis.* **13**, 1–10.
- 679 Schäfer, C., Rosenblum, M. G., Abel, H.-H. & Kurths, J. 1999 Synchronization in the human
680 cardiorespiratory system. *Phys. Rev. E* **60**, 857–870.
- 681 Strogatz, S. H. 2003 *Sync: the emerging science of spontaneous order*. New York, NY: Hyperion
682 Press.
- 683 Timme, M., Wolf, F. & Geisel, T. 2002 Coexistence of regular and irregular dynamics in
684 complex networks of pulse-coupled oscillators. *Phys. Rev. Lett.* **89**, 258701. (doi:10.1103/
685 PhysRevLett.89.258701)
- 686 Zumdieck, A., Timme, M., Geisel, T. & Wolf, F. 2004 Long chaotic transients in complex networks.
Phys. Rev. Lett. **93**, 244103–244104. (doi:10.1103/PhysRevLett.93.244103)

Journal: PHILOSOPHICAL TRANSACTIONS OF THE ROYAL SOCIETY A

Article id: RSTA20090085

Article Title: Experimental results on synchronization times and stable states in locally coupled light-controlled oscillators

First Author: Nicolas Rubido

Corr. Author: Cecilia Cabeza

AUTHOR QUERIES - TO BE ANSWERED BY THE
CORRESPONDING AUTHOR

The following queries have arisen during the typesetting of your manuscript. Please answer these queries by marking the required corrections at the appropriate point in the text.

| | | |
|-----|--|--|
| AQ1 | Please note that the reference citation & Manrubia <i>et al.</i> (2004) has been changed to Manrubia <i>et al.</i> (2003) and Morgul (1998) has been changed to Morgul (2008) with respect to the reference list provided. | |
| AQ2 | Please note that the reference citation Kreuz (2007) has been changed to Kreuz <i>et al.</i> (2007) with respect to the reference list provided. | |